J Appl Electrochem (2013) 43:101–106
DOI 10.1007/s10800-012-0486-1

SHORT COMMUNICATION

On the co-adsorption process of sodium dodecyl sulfate and sodium dodecylbenzenesulfonate on a 1-decanethiol-functionalized Au electrode, as a corrosion inhibiting mimic process

Claudio Fontanesi · Giulio Camurri · Francesco Tassinari

Received: 26 July 2012 / Accepted: 26 September 2012 / Published online: 12 October 2012

Abstract The co-adsorption of sodium dodecyl sulfate (SDS) and sodium dodecylbenzenesulfonate (SDBS), on the 1-decanethiol self-assembled monolayer (SAM)-functionalized polycrystalline gold surface, is investigated by electrochemical techniques. The peak current (cyclic voltammetry) and charge transfer resistance (impedance spectra) variations are measured, concerning the $[Fe(CN)_6]^{3-}/[Fe(CN)_6]^{4-}$ couple redox process. SDBS is found to yield a more efficient inhibiting barrier (towards the charge transfer process), when compared to the SDS one. Thus, it is suggesting that a higher tendency of SDBS to be co-adsorbed within the 1-decanethiol SAM with respect to SDS.

Keywords Adsorption · Impedance · SDS · SDBS

1 Introduction

Metal corrosion is one of the main problems of oil and gas industries, costing every year billions of dollars of maintenance [1]. Modern technologies used in fighting corrosion include physical barrier films, chemical scavengers and chemical passivation of the metal surface. Self-assembled monolayers (SAMs) are being studied as part of a possible solution for corrosion problems for various metals [2, 3], acting as an adhesion promoter for thin polymer films or as a proper coating, depending on the structure of the molecule [4]. Thiol SAMs are extensively studied for this kind of application, especially for the surface protection of mild steel [5]. Another way to protect the surface is by the use of surfactants that can form a protecting layer on the metal. The film formation mechanism, in the case of surfactants, can be different from the one characterizing SAMs formation. In general, the adsorption of surfactants does not imply a substrate/adsorbate covalent bond formation, but rather hydrophobic and hydrophilic interactions. This implies that the surfactant concentration plays a major role for the effectiveness of the protective layer, since a critical micelle concentration is required to form at least a monolayer [6]. Note that, the level of corrosion inhibition, the lowering of the double layer capacitance, and in general, the influence of co-adsorption of other species on the metal-coated thiol monolayer are essentially related to a number of microdefects of the adsorbed layer itself [7]. In fact, when the barrier properties of the coated electrode are high, the redox features of any active species in solution are ruled by the electron tunneling [8, 9], while the existence of a low degree of packing in the thiol layer (that is the presence of the so called "pinholes") and/or the defective structure anyway showed by the underlying metal structure, lead to a marked decrease of the barrier affecting the mechanism of the electron transfer between redox solutes and the metal electrode surface [10–12]. Now, the features of the thiol SAMs in water solution can be studied in relation to the molecular structure of the thiol derivatives: a different chain length of the alkanethiols should affect in a direct way the thickness of the electrical double-layer, which is formed by the chemisorbed thiol molecules with the sulfur atom interacting with the surface and leaving the hydrocarbon chain oriented towards the solution. In this work, the effect of using both SAM and surfactant in one system

C. Fontanesi (✉) · F. Tassinari
Department of Chemistry and Geology, University of Modena and Reggio Emilia, Modena, Italy
e-mail: claudio.fontanesi@unimore.it

G. Camurri
LAMP S. Prospero SPA, Via della pace, 25/A, 41030, S. Prospero S/S, Modena, Italy

is investigated, following the idea of taking advantage of the properties of the surfactant to maximize the protective action of the thiol SAM. The 1-decanethiol is here considered and studied with and without the presence, in solution, of two different surfactants: sodium dodecyl sulfate (SDS) and sodium dodecylbenzenesulfonate (SDBS). In this way, the presence of defects within the 1-decanethiol SAM can be modified by the co-adsorption of these amphiphilic surfactants on the thiol SAM via the chain–chain interaction, which is of hydrophobic nature. The differences found in the co-adsorption efficiency of SDS and SDBS have been related to the different molecular structure of the two surfactants. The protective efficiency of the three systems here considered (i.e., 1-decanethiol SAM, 1-decanethiol SAM with co-adsorbed SDS, and 1-decanethiol SAM with co-adsorbed SDBS) is studied and compared using the $Fe(CN)_6^{3-/4-}$ redox couple exploited as an electrochemical probe towards the conductivity of the surface. To this end, cyclic voltammetry (CV) and electrochemical impedance spectroscopy (EIS) measurements were carried out.

2 Experimental

2.1 Materials

1-Decanethiol, potassium hexacyanoferrate(II) trihydrate, and potassium hexacyanoferrate(III) were purchased from Aldrich and used without further purification. SDS was purchased from BIO-RAD laboratories and SDBS from Aldrich. All the other reagents were analytical grade and used as received. All solutions were prepared with reagent grade water purified by Milli-QII (Millipore, USA).

2.2 Au/SAM preparation

A gold electrode with a diameter of 3.0 mm (Area: 0.07 cm^2) was used as the working electrode. Prior to use, the surface was polished carefully with 0.05 μm alumina slurry and then sonicated in distilled water; after the polishing step, the electrode is treated with piranha solution (7:3 V/V concentrated H_2SO_4/H_2O_2 (Caution: piranha solution reacts violently with many organic materials and should be handled with great care) for 15 min at room temperature and rinsed with water. Then, the gold surface was subjected to cyclic potential sweeps between −0.2 and 1.2 V in H_2SO_4 until a stable cyclic voltammogram was obtained. Subsequently, the surface functionalization is obtained by dipping in a 0.1 mM 1-decanethiol ethanol solution for 48 h. Finally, the electrode was washed with ethanol and re-distilled water and dried with a stream of nitrogen. Electrochemical measurements were carried out immediately after the preparation of the functionalized electrodic surface.

All the electrochemical measurements were carried out at 298 ± 1 K, in deareated solutions.

2.3 Electrochemical measurements

Electrochemical experiments were performed in a three electrodes conventional electrochemical cell. A Pt plate electrode and an Ag/AgCl (saturated KCl) electrode were used as counter and reference electrodes, respectively. The apparatus used for EIS measurements was composed by a Solartron Co. Model 1250 frequency response analyzer connected with a Model 1286 potentiostat via an IEEE-interface (National Instruments, Austin, TX, USA). A sinusoidal potential modulation of 5 mV amplitude was superimposed on a fixed d.c. potential. The capacitance voltage behavior was measured by recording the current response to an a.c. signal with a peak-to-peak amplitude of 5 mV at a frequency of 25 Hz. Impedance spectra were obtained scanning the 100 kHz ÷ 1 mHz frequency range. CV measurements were performed using a CHI 660A Electrochemical Workstation (CH Instruments, USA).

2.4 Calculations

The geometries of both SDS and SDBS were full optimized using the PM3 hamiltonian. The solvent effect was calculated using the SM5.42R model. The solvation free energy in water was calculated at the SM5.42R/PM3//6-31g* level, with CM2 class IV charges. Calculations were performed using the GAMESOL program [13].

3 Results and discussion

Figure 1 shows the cyclic voltammogram of a 3.8 mM $[Fe(CN)_6]^{3-}/[Fe(CN)_6]^{4-}$ in 0.4 M KNO_3 aqueous solution, a freshly prepared gold electrode is the working electrode. Two diffusion-limited current peaks are present, the standard potential is 0.220 V versus Ag/AgCl, with a 0.06 V peak-to-peak separation, in close agreement with data present in the literature [14].

It is well known that the voltammetric response depends on the nature of the electrode/solution interface. The adsorption of long-chain *n*-alkanethiol compounds on the electrodic surface, leading to non-conducting SAM formation, induces a widening in the peak-to-peak potential separation and a lowering of the peak current. Moreover, the peak current and the peak-to-peak separation are also affected by the presence of "defects" in the adsorbed layer: low degree of order in the SAM itself, areas not covered by

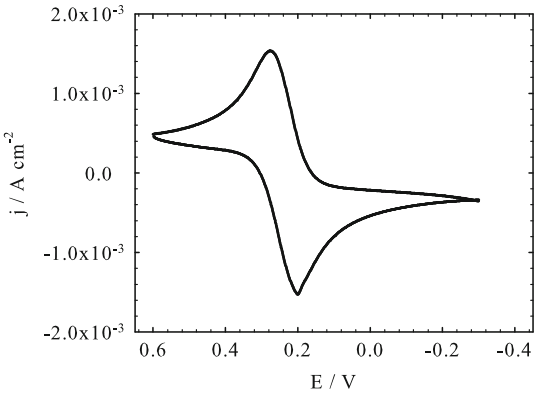

Fig. 1 Cyclic voltammogram, 3.8 mM $[Fe(CN)_6]^{3-}/[Fe(CN)_6]^{4-}$, in 0.4 M KNO_3 aqueous solution, gold bare surface. Scan rate 0.1 V s^{-1}, electrode area 0.07 cm^2

the organic adsorbate, i.e., the presence of the so-called "pin-holes."

Figure 2 shows the CVs of a 3.8 mM $[Fe(CN)_6]^{3-}/[Fe(CN)_6]^{4-}$ in 0.4 M KNO_3 aqueous solution, as a function of the surfactant concentration. Figure 2a and b report the CVs relevant to SDS and SDBS, respectively; the working electrode is a 1-decanethiol SAM-functionalized polycrystalline gold surface. Note that, an ideally well-ordered 1-decanethiol SAM should work by itself as an inhibitor of the faradaic process, due to its insulating electrical features. Nonetheless, SAM structures are characterized by the presence of surface defects often referred as pin-holes, see for instance refs. [9, 12] and references therein cited. Also in our case, the 1-decanethiol-functionalized polycrystalline gold surface is not an ideal defect-free structure, as can be inferred by inspection of the $C = 0$ M (i.e., the surfactant free solution) CV curve shown in Fig. 2. The latter CV is characterized by the presence of two broad current peaks at −0.28 and at 0.6 V: the, not negligible, peak current is about 0.4 mA cm^{-2}, and 0.88 V is the peak–to–peak potential separation (the CV recorded on the bare Au surface features 1.5 mA cm^{-2} peak current and 0.06 V peak–to–peak separation, Fig. 1). The insulating properties of the 1-decanethiol SAM can be improved by adding a suitable surface active species in the aqueous solution. Figure 2a shows CV curves obtained when SDS is added to the solution at three different concentrations: 0.1, 1.0, and 5.0 mM. SDS is co-adsorbed within the SAM of the 1-decanethiol, and the current diminishes at increasing the SDS concentration.

Figure 2b shows the effect produced by the addition in solution of SDBS, again at three different concentrations: 0.1, 0.5, and 1.0 mM. Note that, Fig. 2b CV curves (SDBS present in solution) are now almost independent of the surfactant concentration, and the current is virtually zero. This result strongly indicates that SDBS is more strongly

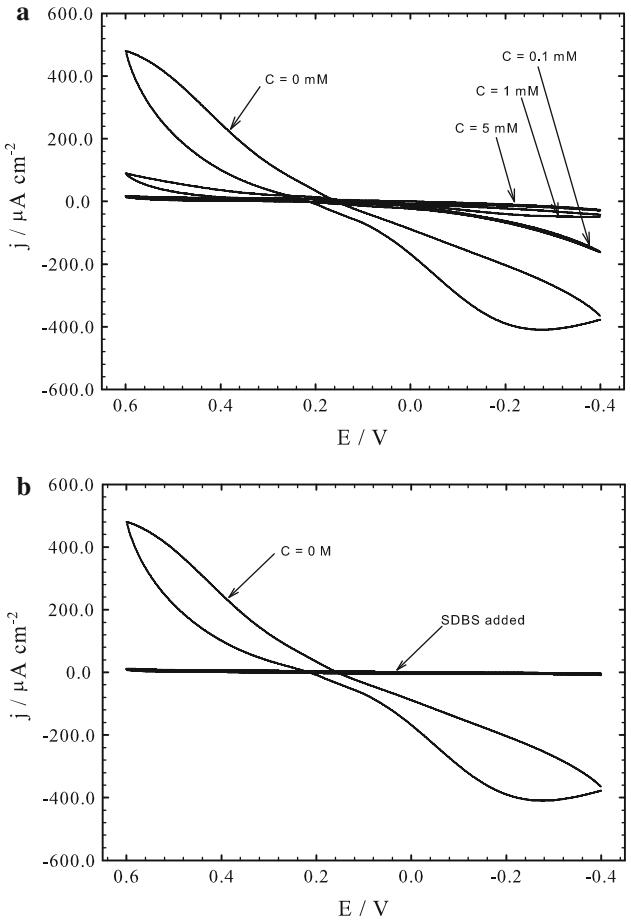

Fig. 2 **a** Cyclic voltammograms of a gold electrode functionalized with a 1-decanethiol SAM, in solution of 3.84 mM $[Fe(CN)_6]^{3-}/[Fe(CN)_6]^{4-}$. Scan rate 0.1 V s^{-1}, electrode area 0.07 cm^2. SDS concentration: 0, 0.1, 1.0, and 5.0 mM. **b** Cyclic voltammograms of a gold functionalized with a 1-decanethiol SAM, in solution of 3.84 mM $[Fe(CN)_6]^{3-}/[Fe(CN)_6]^{4-}$. Scan rate 0.1 V s^{-1}, electrode area 0.07 cm^2. SDBS concentration: 0, 0.1, 0.5, and 1.0 mM

co-adsorbed in comparison to SDS, eventually featuring a more efficient inhibiting activity.

This result is obtained despite the larger solubility of SDBS with respect to SDS (the free energy of solvation relevant to the process of solution in water from the vacuum phase was calculated using the GAMSOL program RHF/6-31g*: SDS = −84.7 kcal mol^{-1}, SDBS −96.3 kcal mol^{-1}, SDBS −96.3 kcal mol^{-1}), note that in general a low solubility is associated to strong adsorption capability and vice-versa [15]. So, the "driving–force" underlying the greater affinity of SDBS in the interaction with the 1-decanethiol SAM can be attributed to the larger ability of the benzyl moiety to delocalize the negative charge of the anion, while, in the case of SDS, the negative charge is essentially localized on the $-O-SO_2-O$ moiety (see the values in Table 1, and compare the molecular structures in Chart 1). This different feature regarding the delocalization

SDBS

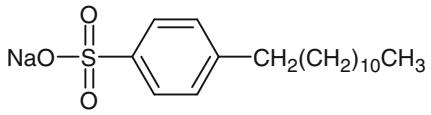

SDS

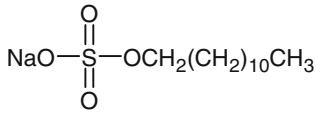

Chart 1

of the anionic negative charge yields different results: (i) the SDBS anion is more stable from the energetic point of view, so inducing a higher solubility with respect to SDS (ii) the hydrophilic head-groups of SDBS are affected by a weaker electrostatic reciprocal repulsion, and this represents a leading energetic effect in the close packing experienced by the molecules in the adsorbed state (iii) the presence of the aromatic group in the frame of SDBS, enhances the hydrophobic character of the amphiphilic moiety improving the attractive nature of the interaction between the thiol and surface-active molecules.

Then, owing to the remarkable inhibiting activity associated to the SDBS co-adsorption, EIS measurements were carried out to further characterize the Au/1-decanethiol SAM/SDBS/solution interface. Figure 3 shows the changes affecting the ac impedance spectra of a 1-decanethiol-functionalized gold electrode in solution of $[Fe(CN)_6]^{3-}$/$[Fe(CN)_6]^{4-}$ containing SDBS at three different concentrations, 0.1, 0.5, and 1.0 mM, the impedance spectrum features a single arc in the complex plane representation (a parametric Cartesian plane where the imaginary part of the impedance, z_i, is reported versus the real part of the impedance, z_r, as a function of the frequency of the perturbing a.c. signal).

Impedance spectra shown in Fig. 3 are fitted using a three elements equivalent circuit: a resistance, *R*1, in series to a parallel (*R*2 *Q*) net (Randles equivalent circuit), as represented in Fig. 4 [16]. This is the typical choice used to rationalize impedance spectra relevant to electrochemical systems involving a charge transfer process at the electrode/SAM/solution interface. The addition of SDBS causes *R*2 to increase and the Warburg-line (which is found if "pin-holes" are present in the SAM) to disappear, *R*2 is the electric circuit element representative of the charge transfer kinetics, i.e., larger *R*2 values are associated to slower kinetics and smaller currents [16].

The results of the fitting procedure [17] are reported in Table 2. A rather satisfactory agreement is found between experimental and calculated impedance spectra. *R*1 can be considered representative of the bulk solution resistance,

Table 1 Calculated net charge values (PM3 method)

	SO_3 moiety/*e*	O/*e*	Phenyl group/e	$CH_3(CH_2)_{11}$ moiety/*e*
SDS	−0.47	−0.64		+0.11
SDBS	−0.52		−0.52	+0.04

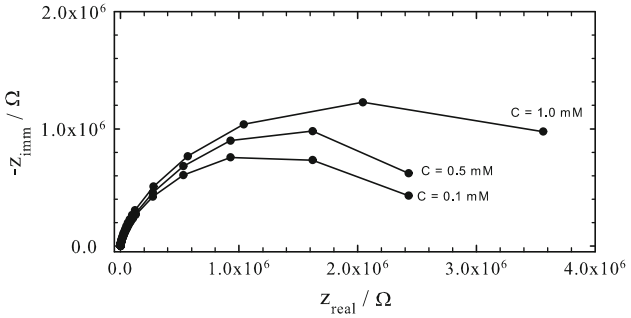

Fig. 3 Impedance spectra of a gold electrode functionalized with a 1-decanethiol SAM, in solution of 3.84 mM $[Fe(CN)_6]^{3-}$/$[Fe(CN)_6]^{4-}$. Electrode potential (open circuit potential) 0.22 V. SDBS concentration: 0.1, 0.5 and 1.0 mM

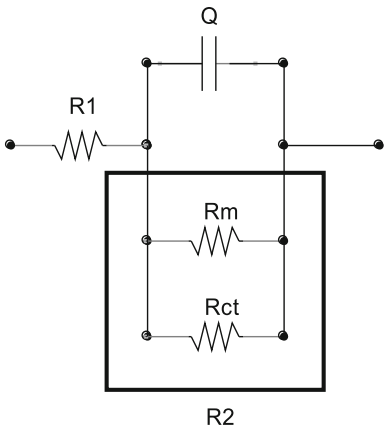

Fig. 4 Electrical equivalent circuit used to model experimental impedance spectra

Q can be considered representative of the double layer interfacial capacitance, this because the value of *n* (the specific generalized capacitance element) is close to 1 [16]. However, the most interesting result rests on the evidence that *R*2, which can be considered representative of the apparent electron transfer resistance, increases with increasing the concentration of SDBS, the improved inhibitory action suggests a strong co-adsorption of SDBS.

For sake of comparison, the structure of the 1-decanethiol SAM-functionalized gold surface has been characterized too, again by means of EIS measurements. Figure 5 shows impedance spectra of 1-decanethiol SAM-functionalized gold electrode at various concentrations of the $[Fe(CN)_6]^{3-}$/$[Fe(CN)_6]^{4-}$ redox couple. The impedance

Table 2 Results of the fitting procedure for the data in Figs. 3 (a) and 5 (b), the equivalent circuits are shown in Fig. 4

	$R1/\Omega$	$R2 \times 10^5/\Omega\ \mathrm{cm}^{-2}$	Q / μF cm^{-2}	n
(a) c^A				
0.1	602	608	2.7	0.88
0.5	432	745	2.9	0.87
1.0	426	887	2.9	0.88
(b) c^B				
1	119	4.19	1.4	0.82
2	112	3.89	1.5	0.87
3	100	3.68	1.4	0.85
3.8	119	3.23	1.2	0.76
5.0	92	3.14	1.2	0.77

[A] (SDBS)/ mM

[B] $[Fe(CN)_6]^{3-/4-}$/mM

spectra are all characterized by the presence of a single arc in the complex-plane, which can be attributed to an almost pinhole-free monolayer. Again, the experimental electrochemical response was modeled on the basis of the equivalent circuit shown in Fig. 4. Table 2 summarizes the results of the fitting procedure. Note that $R1$ is almost constant, about 100 Ω , Q values are, again, almost independent of the redox couple concentration (resulting in a rather low value of capacity $\simeq 1.3$ μF cm^{-2}). Figure 6 sets out $R2^{-1}$ values as a function of the $[Fe(CN)_6]^{3-}$/$[Fe(CN)_6]^{4-}$ concentration [9, 11]. According to the model proposed by Hu-Lin Li and Jie Xu [9], the apparent resistance element $R2$ is assumed to consist of two parallel resistances, R_{ct} and R_m (compare Fig. 4): R_{ct} represents the electron transfer kinetics contribution and R_m is considered representative of the SAM resistance (assumed to be independent of the concentration of the redox species [9]): $1/R2 = 1/R_m + 1/R_{ct}$ [18]. Within this view, the redox current density, at a fixed potential, should decrease exponentially with the monolayer thickness:

$$j = j_0 \exp(-\beta d_e)$$

where j_0 is the current density for the bare electrodic surface, β the electronic tunneling coefficient, and d_e the thickness of the SAM. Moreover, $j_0 = nFk_0c$ where n number of exchanged electrons in the redox process, F Faraday constant, k_0 apparent heterogeneous electron transfer constant, c the bulk concentration of the redox couple and $k_0 = k_S \exp(-\alpha nF\eta/RT)$ [9]. At the open circuit potential, $\eta = 0$ V [11, 12, 19]:

$$j = (RT/nF)(1/R_{ct})$$

and then:

$$1/R_{ct} = (n^2F^2k_S/RT)c \exp(-\beta d_e)$$

eventually:

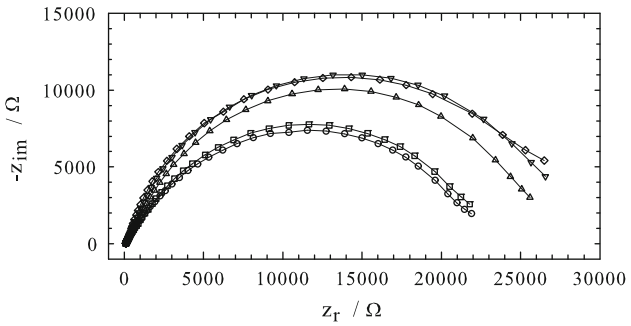

Fig. 5 Impedance spectra of a gold electrode functionalized with a 1-decanethiol SAM, in solution of 1.0 (*triangle down*), 2.0 (*diamond*), 3.0 (*triangle up*), 3.8 (*square*), 5.0 (*circle*) mM $[Fe(CN)_6]^{3-}$ / $[Fe(CN)_6]^{4-}$. Electrode potential (open circuit potential) 0.22 V

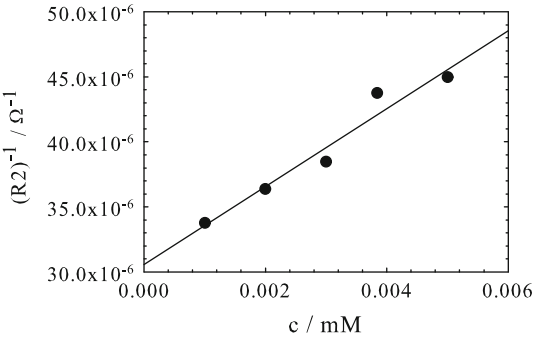

Fig. 6 $1/R2$ versus c plot of a gold electrode functionalized with a 1-decanethiol SAM, in solution of 1.0, 2.0, 3.0, 3.8, 5.0 mM $[Fe(CN)_6]^{3-}/[Fe(CN)_6]^{4-}$

$$1/R2 = 1/R_m + (n^2F^2k_S/RT)c \exp(-\beta d_e)$$

where $k_S = 0.026$cm s^{-1} [18], $\beta = 1.02/CH_2$ [9]. Thus, from the slope of the $1/R2$ versus c plot (Fig. 6), the apparent effective thickness of the monolayer film can be determined. In the present case, $R_m = 4.5 \times 10^5\ \Omega\,\mathrm{cm}^{-2}$ and $d_e/CH_2 = 9.8$ values are obtained. The latter result suggests a SAM thickness in agreement with the number of CH_2 groups present in the 1-decanethiol.

4 Conclusions

The co-adsorption process of SDS and SDBS surfactants on a 1-decanethiol SAM has been characterized using voltammetry and impedance spectroscopy techniques. It is observed that the charge transfer resistance increases as the concentration of the surface active species is increased, as previously found in the case of SDS co-adsorbed on an octadodecanethiol SAM [12]. The greater charge transfer inhibiting ability of SDBS, compared to that of SDS, suggests that SDBS is more strongly co-adsorbed than SDS. The apparent effective thickness of the 1-decanethiol

SAM has been assessed on the basis of the model proposed in refs. [9] and [11], and it is found in agreement with the formation of one monolayer.

As a whole, the adsorption of a suitable organic compound (in this case the 1-decanethiol) followed by the co-adsorption of a surface active species (in this paper SDS and SDBS are compared) appears as an interesting strategy to obtain a synergetic enhancement effect for an effective metal protection. Further development of this approach could involve the implementation of the same general strategy, but exploiting electrochemical grafted organics [20–23] as the substrate for the surfactant co-adsorption.

Acknowledgments This research was supported by the Italian Ministry of University and Research (MIUR) through PRIN 2008 (Project 2008N7CYL5) in charge of the Prof. M. L. Foresti (national co-ordinator).

References

1. Koch GH, Koch GH, Brongers MPH, Thompson NG, Virmani YP, Payer JH (2007) http://www.nace.org/uploadedFiles/Publications/ccsupp.pdf
2. Itoh M (1994) J Electrochem Soc 141(8):2018
3. Grundmeier G, Reinartz C, Rohwerder M, Stratmann M (1998) Electrochim Acta 43(1):165
4. Aradilla D, Azambuja D, Estrany F, Iribarren JI, Ferreira CA, Alemn C (2011) Polym Chem 2:2548
5. Solmaz R, Kardas G, Ulha M, Yazc B, Erbil M (2008) Electrochim Acta 53(20):5941
6. Free ML (2002) Corros Sci 44(12):2865
7. Finklea HO (1996) Electroanal Chem 19:109
8. Nahir TM, Bowden EF (1994) Electrochim Acta 39(16):2347
9. Xu J, Li HL, Zhang Y (1993) J Phys Chem 97(44):11497
10. Finklea HO, Hanshew DD (1992) J Am Chem Soc 114(9):3173
11. Cui X, Jiang D, Diao P (1999) J Electroanal Chem 470(1):9
12. Cui X, Jiang D, Diao P, Li J, Jia Z, Tong R (2000) Colloids Surf A 175(1−2):141
13. Xidos DJ, Li J, Zhu T, Hawkins DG, Chuang Y-Y, Fast PL, Liotard DA, Rinaldi D, Cramer CJ, Truhlar DG (2001) GAMESOL version 3.0, University of Minnesota, Minneapolis, based on the General Atomic and Molecular Electronic Structure System (GAMESS) as described in Schmidt MW, Baldridge KK, Boatz JA, Elbert TS, Gordon MS, Jensen JH, Koseki S,Matsunaga N, Nguyen KA, Su SJ, Windus TL, Dupuis M, Montgomery JA (1993) J Comp Chem 14:1347
14. Bard AJ, Faulkner LR (2001) Electrochemical methods. Fundamentals and applications, 2nd edn. Wiley, New York
15. Damaskin BB, Petrii OA, Batrakov VB (1971) Adsorption of organic compounds on electrode. Plenum Press, New York
16. Boukamp BA (1986) Solid State Ion 18(19):136
17. FRA (2000) Autolab, version 4.8. Eco Chemie, Utrecht
18. Sabatani E, Cohen-Boulakia J, Bruening M, Rubinstein I (1993) Langmuir 9(11):2974
19. Tian Z (1984) Method for electrochemical research. Science Press, Beijing
20. Yu SSC, Downard AJ (2007) Langmuir 23(8):4662–4668
21. Vase KH, Holm AH, Norrman K, Pedersen SU, Daasbjerg K (2007) Langmuir 23(7):3786–3793
22. Fontanesi C, Bortolotti CA, Vanossi D, Marcaccio M (2011) J Phys Chem A 115(42):11715–11722
23. Vanossi D, Benassi R, Parenti F, Tassinari F, Giovanardi R, Florini N, De Renzi V, Arnaud G, Fontanesi C (2012) Electrochim Acta doi:10.1016/j.electacta.2012.04.128